PTEP

Prog. Theor. Exp. Phys. **2022** 041D01(9 pages)
DOI: 10.1093/ptep/ptac055

New constraints on the neutron-star mass and radius relation from terrestrial nuclear experiments

Hajime Sotani [1,2,⋆], Nobuya Nishimura[1,3,4], and Tomoya Naito[3,5]

[1] *Astrophysical Big Bang Laboratory, RIKEN, Saitama 351-0198, Japan*
[2] *Interdisciplinary Theoretical & Mathematical Science Program (iTHEMS), RIKEN, Saitama 351-0198, Japan*
[3] *RIKEN Nishina Center for Accelerator-Based Science, Saitama 351-0198, Japan*
[4] *Division of Science, National Astronomical Observatory of Japan, Tokyo 181-8588, Japan*
[5] *Department of Physics, Graduate School of Science, The University of Tokyo, Tokyo 113-0033, Japan*
⋆E-mail: sotani@yukawa.kyoto-u.ac.jp

Received February 20, 2022; Revised March 9, 2022; Accepted March 23, 2022; Published March 25, 2022

The determination of the equation of state (EOS) for nuclear matter has been one of the biggest problems in nuclear astrophysics, because the EOS is essential for determining the properties of neutron stars. To constrain the density dependence of the nuclear symmetry energy, several nuclear experiments, e.g., reported by the SπRIT and PREX-II Collaborations, have recently been performed. However, since their uncertainties are still large, additional constraints such as astronomical observations are crucial. In addition, it is interesting to see the effect of their reported values on neutron-star properties. In this study, focusing on a relatively lower-density region, we investigate the allowed area of the neutron-star mass and radius relation by assuming the constraints from SπRIT and PREX-II. Each region predicted by these experiments is still consistent with the allowed area constrained by the various astronomical observations. Our results show that terrestrial nuclear experiments must provide further constraints on the EOS for neutron stars, complementing astronomical observations.

Subject Index E32, D41

1. Introduction

Core-collapse supernovae, which occur at the end of a massive star's life, produce a neutron star (NS) (or a black hole) as a compact remnant. Since the density inside the NS becomes significantly larger than the nuclear saturation density, which must be the densest environment in nature, the nuclear equation of state (EOS) describing NS matter is not yet fixed. So, astronomical observations help us to understand the properties in such a high-density region. For example, the discovery of NSs heavier than $2\,M_\odot$ could rule out some soft EOSs, with which the theoretical maximum mass does not reach the observed mass [1–3]. The observation of gravitational waves from a binary NS merger, GW170817, gives us the constraint on the tidal deformability, which estimates that the $1.4\,M_\odot$ NS radius should be less than 13.6 km [4]. The electromagnetic signals from the NS also give a constraint on the neutron-star mass and radius, although it depends on the theoretical models [5–7]. In this way, NS observations essentially give us information and/or constraints on a relatively high-density region.

As traditionally performed, on the other hand, terrestrial particle-accelerator experiments are still crucial to obtain information on the physics of nuclear matter. Owing to the nuclear

saturation properties, one may easily constrain the EOS around the nuclear saturation density. In fact, several experiments have been performed to determine the nuclear saturation parameters, especially focusing on nuclear symmetry energy. Here, the symmetry energy is roughly the difference between the energy for symmetric nuclear matter and that for pure neutron matter. This is one of the key properties for constructing the EOS for NS matter because NS matter is very neutron-rich under the β-equilibrium state. Even so, access to the symmetry energy via terrestrial experiments is relatively more difficult than that for other nuclear properties, because the stable atomic nucleus on the Earth is at most $\alpha \simeq 0.3$, where α is an asymmetry parameter. We note that $\alpha = 0$ and 1 correspond to symmetric nuclear matter and pure neutron matter, respectively.

Recently, new experiments in two large facilities have reported a constraint on the density dependence of symmetry energy, L (see Eq. (3) for a definition); $42 \leq L \leq 117$ MeV by the Radioactive Isotope Beam Factory (RIBF) at RIKEN in Japan (SπRIT; see, e.g., Ref. [8]) and $L = 106 \pm 37$ MeV obtained by the polarized-electron scattering done at the Thomas Jefferson National Accelerator Facility in Newport News, Virginia, USA (PREX-II) [9,10]. Compared to the previous L values, the PREX-II result suggests a significantly large L, while the SπRIT result also supports a relatively large value. On the other hand, the constraint through the polarized-proton scattering experiment performed at the Research Center for Nuclear Physics (RCNP), Osaka University, Japan [11] is more or less consistent with the other predictions obtained so far, even though the same nuclear property, i.e., the neutron-skin thickness, has been measured at RCNP and PREX-II, but via a different probe. So, current terrestrial experiments cannot solely determine the value of L, so astronomical observations must be important; this is a qualitatively different approach and covers higher nuclear densities. In the context of astrophysics, constraints on L become more informative if they are interpreted on the NS mass and radius relation, which can be easily compared with other astronomical constraints by X-ray and gravitational-wave observations.

In this study, therefore, we concretely show the allowed region in the NS mass and radius relation, based on the two new constraints on L (SπRIT and PREX-II) and another experimental constraint previously obtained (RCNP). The NS mass and radius curves theoretically constructed with the EOSs should be compared with these constraints, as well as the several astronomical restrictions given by X-ray and gravitational-wave observations. We discuss the consistency in the constraints between the nuclear experiments and astronomical observations.

2. EOS and nuclear saturation parameters

In order to construct the NS models, one has to prepare the EOS for NS matter. For any nuclear EOSs, the bulk energy per nucleon for nuclear matter with zero temperature, w, is written as a function of the baryon number density $n_{\rm b}$ and the asymmetry parameter α as

$$w(n_{\rm b}, \alpha) = w_{\rm s}(n_{\rm b}) + \alpha^2 S(n_{\rm b}) + \cdots , \tag{1}$$

where $n_{\rm b}$ and α are defined by $n_{\rm b} = n_n + n_p$ and $\alpha = (n_n - n_p)/n_{\rm b}$ with the neutron number density n_n and the proton number density n_p. In this expansion, $w_{\rm s}$ and S correspond to the energy per nucleon of symmetric nuclear matter, i.e., $w_{\rm s} = w(n_{\rm b}, 0)$, and the density-dependent symmetry energy given by $S(n_{\rm b}) = \partial w/\partial \alpha^2|_{\alpha=0}$, respectively. Additionally, $w_{\rm s}$ and S can be expanded as a function of $u \equiv (n_{\rm b} - n_0)/(3n_0)$ with the saturation density of symmetric nuclear matter, n_0, as

$$w_{\rm s}(n_{\rm b}) = w_0 + \frac{K_0}{2}u^2 + \frac{Q_0}{6}u^3 + \cdots , \tag{2}$$

$$S(n_{\rm b}) = S_0 + Lu + \frac{K_{\rm sym}}{2}u^2 + \frac{Q_{\rm sym}}{6}u^3 + \cdots . \tag{3}$$

The coefficients are referred to as the nuclear saturation parameters. In particular, among these parameters, the saturation parameters in the lowest order, such as n_0, w_0, K_0, S_0, and L, are the most important, being strongly associated with the properties of the atomic nuclei in nature, and are constrained via terrestrial experiments. Even so, n_0, w_0, and S_0 are relatively well constrained, while K_0 and L are more difficult to constrain. This is because one can easily obtain the nuclear information around the saturation density, owing to the nuclear saturation properties, whereas, to obtain parameters associated with the density derivative, such as K_0 and L, it is necessary to obtain information on nuclear matter properties at various densities.

Thus, in this study, we focus on K_0 and L, where n_0, w_0, and S_0 must be tuned in such a way that the properties of stable nuclei should be reproduced by any EOSs. Via the data for the isoscalar giant monopole resonance in ^{208}Pb and ^{90}Zr, K_0 is constrained in the range of $K_0 = 240 \pm 20$ MeV [12], which seems to be a conservative constraint [13]. On the other hand, there have been several attempts to constrain L, which tell us that L should be in the range of $L \simeq 60 \pm 20$ MeV [14,15]. Nevertheless, the recent experiments seem to predict a larger value of L than the previous constraints, as mentioned in the next section.

3. Experimental constraints

In this study, we especially focus on two recent terrestrial nuclear experiments, i.e., SπRIT and PREX-II, together with RCNP. SπRIT is the experiment with the isotope beams provided by the RIBF at RIKEN in Japan, where beams of ^{132}Sn, ^{124}Sn, ^{112}Sn, and ^{108}Sn were used to bombard the ^{124}Sn and ^{112}Sn targets. Throughout such reactions, Δ isobars were produced, which decay to nucleons with the emission of pions. The ratio of the production rate of positively charged pions, π^+, to that of negatively charged ones, π^-, allows one to constrain L as $42 \le L \le 117$ MeV with 1σ accuracy [8]. PREX-II is the experiment after PREX (the ^{208}Pb Radius Experiment) at the Thomas Jefferson National Accelerator Facility in Virginia. In the PREX/PREX-II experiments, first, the scattering cross sections of spin-up polarized electrons $\sigma_\uparrow$ and spin-down ones $\sigma_\downarrow$ in ^{208}Pb are measured. Then, using the parity-violating asymmetry $(\sigma_\uparrow - \sigma_\downarrow)/(\sigma_\uparrow + \sigma_\downarrow)$, one can estimate the neutron root-mean-square radius and, accordingly, the neutron-skin thickness, whose values are $\Delta r_{np} = 0.33^{+0.16}_{-0.18}$ fm in PREX [16] and $\Delta r_{np} = 0.283 \pm 0.071$ fm in PREX-II [9]. By using the data for neutron-skin thickness, the value of L is constrained to be $L = 106 \pm 37$ MeV in PREX-II with 1σ accuracy [10]. We remark that, soon after the report of PREX-II, a reanalysis was done, using the same data for the parity-violating asymmetry in PREX-II, which predicted $\Delta r_{np} = 0.19 \pm 0.02$ fm and L as $L = 54 \pm 8$ MeV [17].

In addition to the above two constraints on L derived by SπRIT and PREX-II, we also consider the experiment at the RCNP, where the neutron-density distributions of $^{204,\,206,\,208}$Pb were measured via polarized-proton elastic scattering, and the neutron-skin thickness especially for ^{208}Pb was deduced to be $\Delta r_{np} = 0.211^{+0.054}_{-0.063}$ fm [11]. It is theoretically known that the neutron-skin thickness is strongly correlated with the slope parameter L [18] as

$$\Delta r_{np}\ ({\rm fm}) = 0.101 + 0.001\,47L, \tag{4}$$

where L is considered in units of MeV, and thus one can extract the constraint on L as $32 \leq L \leq 112$ MeV.

In Fig. 1, we show the constraint on L obtained by the nuclear experiments focused on in this study together with the previous constrains by updating the figure shown in Ref. [14]. In this figure, we show the value of L constrained from the nucleon matter calculated with quantum Monte Carlo techniques [19,20]; the neutron-skin thickness for antiprotonic atoms [21,22]; the neutron-skin thickness in p and α scattering [23]; the neutron-skin thickness in p scattering [11,24]; the neutron-skin thickness in the (γ, π^0) reaction [25]; the parity-violating asymmetry (PREX/PREX-II) [9,10,16]; the empirical nuclear model fit [26–28]; the nuclear model fit thorough energy density functionals (EDF) [29–32]; heavy ion collisions [8,33,34]; nuclear giant resonances [35–40]; nucleon optical potentials [41]; compilation analyses [42–44]; and several NS observations [45–47]. The vertical dotted line denotes the constraint on L as $L \gtrsim 20$ MeV with the condition that the pure neutron matter should not have a quasi-bound state [48].

4. Constraints on the NS mass and radius relation

As mentioned before, any EOSs have their own values of K_0 and L, with which in turn each EOS is characterized. Nonetheless, it may be generally difficult to discuss the dependence of the NS mass and radius on two parameters. To solve this difficulty, an auxiliary parameter, η, is proposed [49], which is a combination of K_0 and L given by

$$\eta = (K_0 L^2)^{1/3}. \tag{5}$$

We note that η has been empirically found, where its physical meaning is still uncertain. Thanks to the introduction of η, one can systematically discuss the NS mass and radius with one parameter, directly adopting the experimental data. In practice, the mass M and gravitational redshift $z \equiv (1 - 2GM/Rc^2)^{-1/2} - 1$ for a low-mass NS with the radius R, whose central density ρ_c is less than twice the nuclear saturation density, are expressed as functions of $u_c \equiv \rho_c/\rho_0$ and η, where G, c, and ρ_0 denote the gravitational constant, the speed of light, and the nuclear saturation density, such as

$$M/\mathrm{M}_\odot = 0.371 - 0.820\mathrm{u_c} + 0.279\mathrm{u_c^2} - \left(0.593 - 1.25\mathrm{u_c} + 0.235\mathrm{u_c^2}\right)\eta_{100}, \tag{6}$$

$$z = 0.008\,59 - 0.0619u_c + 0.0255u_c^2 - \left(0.0429 - 0.108u_c + 0.0120u_c^2\right)\eta_{100}, \tag{7}$$

where η_{100} denotes $\eta/(100\,\mathrm{MeV})$ [49]. Combining $M(u_c, \eta_{100})$ and $z(u_c, \eta_{100})$, one can plot the mass and radius for given values of u_c and η. We note that this technique is applicable only for low-mass NSs because additional effects, such as the many-body effect and/or the appearance of additional composition, should be taken into account when the central density becomes somewhat large.

In Fig. 2, we show the resultant constraint on the NS mass and radius relation by adopting the constraints on L obtained from the nuclear experiments discussed in the previous section, together with the constraint on K_0 as $K_0 = 240 \pm 20$ MeV, which correspond to $72.9 \leq \eta \leq 152.7$ MeV for SπRIT, $101.6 \leq \eta \leq 174.5$ MeV for PREX-II, and $60.8 \leq \eta \leq 147.9$ MeV for RCNP. For reference, we also show the NS mass and radius relation as a fiducial region by assuming fiducial values of L and K_0, i.e., $L = 60 \pm 20$ MeV and $K_0 = 240 \pm 20$ MeV, which correspond to $70.6 \leq \eta \leq 118.5$ MeV. The constraints can be put on the bottom-right part in this figure, i.e., for the low-density region, where we consider the NS model whose central density is up to twice the saturation density. Note that the PREX-II reanalysis ($77.5 \leq \eta \leq 100.0$ MeV) is consistent

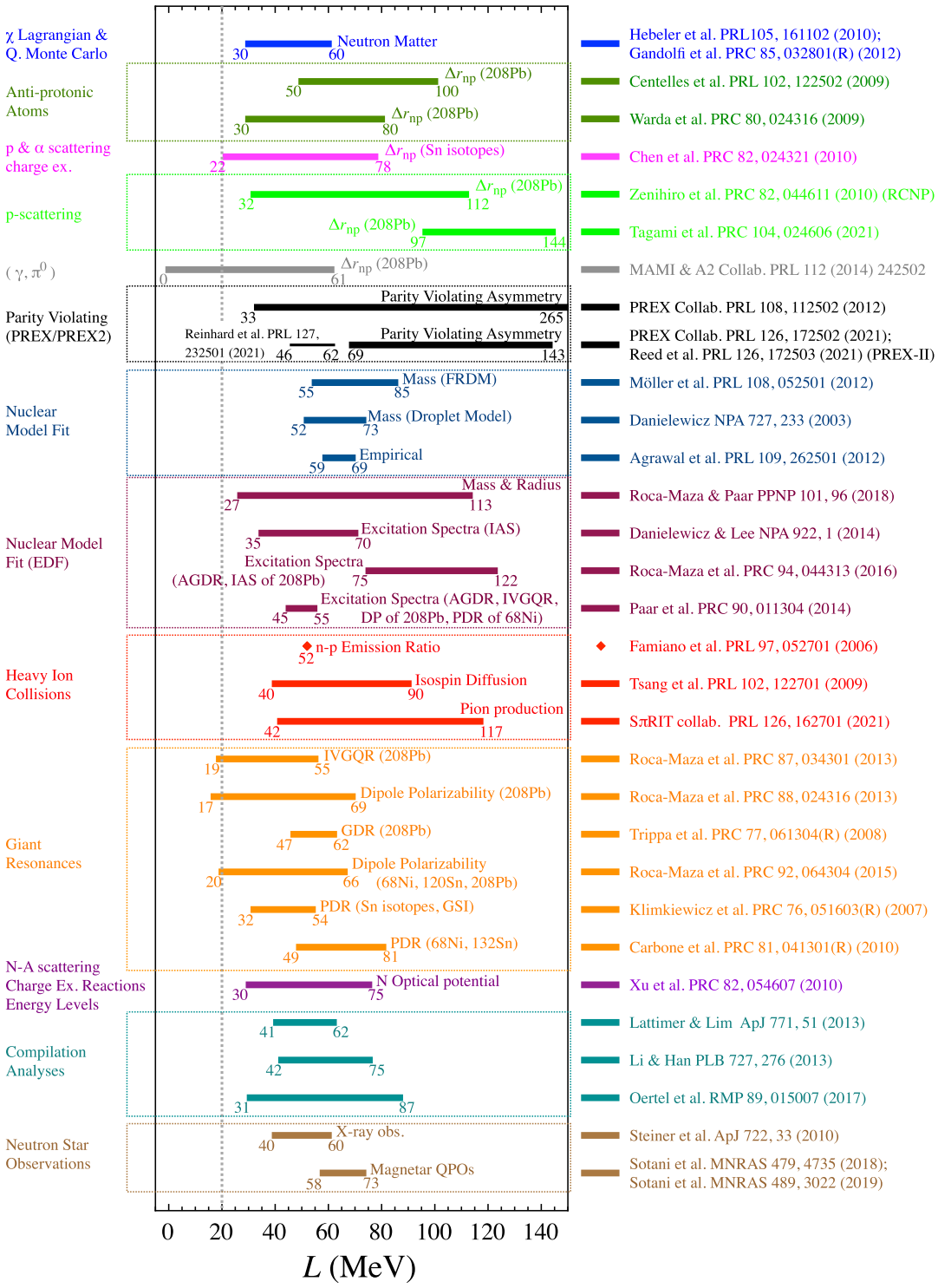

Fig. 1. Constraints on L from various experiments and astronomical observations, updated from the figure in Ref. [14], using the data in Ref. [32] together with the constraints on L discussed in this study. FRDM, IAS, AGDR, IVGQR, DP, PDR, GDR, and Δr_{np} stand for finite-range droplet model, isobaric analog states, anti-analog giant dipole resonance, isovector giant quadrupole resonance, dipole polarizability, pygmy dipole resonance, giant dipole resonance, and neutron-skin thickness, respectively. At the result with PREX-II, the constraint on L with $L = 54 \pm 8$ MeV derived by the reanalysis is also shown (see text for details). The vertical dotted line denotes the lower limit of L constrained from the condition that the pure neutron matter should not have a quasi-bound state [48].

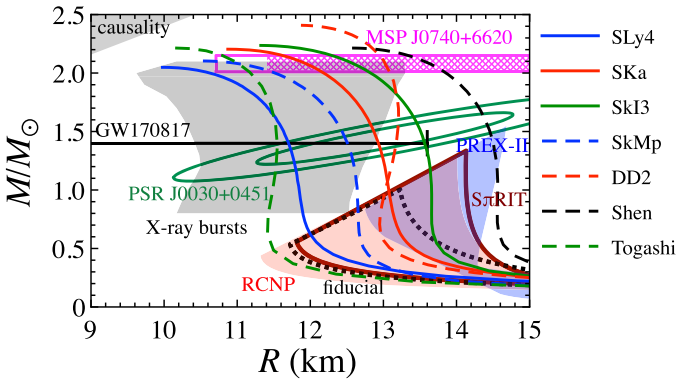

Fig. 2. The constraints derived from the nuclear experiments are put on the bottom-right part, where the constraining region from left to right corresponds to RCNP, SπRIT, and PREX-II. For reference, the fiducial region is also shown, assuming that $L = 60 \pm 20$ MeV and $K_0 = 240 \pm 20$ MeV. In addition, we show the astrophysical and theoretical constraints (see text for details). For reference, NS mass and radius relations constructed with five different EOSs listed in Table 1 are also shown. The constraint from MSP J0740+6620 is shown by the shaded region (68%) and the enclosed region with a solid line (95%).

with the results obtained by RCNP and SπRIT, and thus, hereinafter, it is not explicitly shown. One can eventually constrain the EOS for NS matter, because the NS mass and radius relation predicted by the EOS has to pass through the allowed region shown in Fig. 2.

In order to compare these constraints derived from the experiments, in Fig. 2 we show four different constraints from astrophysical observations and one theoretical constraint. The constraint on the NS radius comes from GW170817 [4]; i.e., the 1.4 $M_\odot$ NS radius should be less than 13.6 km, considering the tidal deformability observed in the gravitational waves from the binary NS merger. The NS with maximum mass observed so far is MSP J0740+6620 [50], whose mass is $M/M_\odot = 2.08 \pm 0.07$. The Neutron star Interior Composition Explorer (NICER) basically gives the constraint on the stellar compactness, M/R, on PSR J0030+0451 by carefully observing the pulsar light curve [6,7]. The resultant constraint is shown by the tilted ellipses, where inner and outer edges correspond to the 1σ (68%) and 2σ (95%) constraints [51]. NICER also gives us the radial constraint on PSR J0740+6620, i.e., $12.39^{+1.30}_{-0.98}$ km [52] and $13.7^{+2.6}_{-1.5}$ km [53]. Through the X-ray burst observations from NSs, one can also constrain the NS mass and radius, as in Ref. [5], where, e.g., the 1.4 $M_\odot$ NS radius lies between 10.4 and 12.9 km. Meanwhile, from the causality, one can exclude the top-left region corresponding to $R < 2.824GM/c^2$ [54]. By comparing the astrophysical and theoretical constraints mentioned here, we can say that all constraints derived from the nuclear experiments are still consistent.

Moreover, in Fig. 2, for reference, we also plot the mass and radius relations for NS models constructed with several EOSs, i.e., EOSs based on the Skyrme-type effective interaction, such as SLy4 [55,56], SKa [57], SkI3 [58], SkMp [59]; the EOS based on the relativistic framework, such as DD2 [60] and Shen [61]; and the EOS constructed with the variational many-body calculation, Togashi [62]. The EOS parameters and the maximum mass for the NS constructed with each EOS are listed in Table 1. The EOSs selected here except for Shen satisfy the astronomical constraints shown in Fig. 2, although SLy4 may be marginal to the constraint from MSP J0740+6620, and they are roughly consistent with the region constrained by three nuclear experiments. We note that, in the present study, Shen is selected for reference because it has been adopted as a standard EOS, even though it has been ruled out from the constraint

Table 1. EOS parameters adopted in this study, K_0, L, and η, and the maximum mass, $M_{\rm max}$, for the NS constructed with each EOS.

EOS	K_0 (MeV)	L (MeV)	η (MeV)	$M_{\rm max}/{\rm M}_\odot$
SLy4	230	45.9	78.5	2.05
SKa	263	74.6	114	2.22
SkI3	258	101	138	2.25
SkMp	231	70.3	105	2.11
DD2	243	55.0	90.2	2.41
Shen	281	111	151	2.17
Togashi	245	38.7	71.6	2.21

from GW170717. Meanwhile, considering the allowed area given by the nuclear experiments (together with the astronomical restrictions), some of the EOSs may be ruled out. For example, the Togashi EOS passes through the lower L boundary, which may be ruled out if the constraints from SπRIT and PREX-II are strictly true. On the other hand, the Shen EOS is consistent only with the higher L (higher M and R) covered by PREX-II, and is inconsistent with some of the astronomical restrictions. Overall, the area covered by SπRIT seems to agree with the other constraints without significant inconsistencies.

5. Conclusion

Terrestrial nuclear experiments must be important for constraining the NS mass and radius relation, especially for a low-density region, and can complement the constraint obtained from astrophysical observations. In this study, we show which region in the NS mass and radius relation is allowed by using the recent constraints on the density dependence of nuclear symmetry energy obtained via SπRIT and PREX-II together with the experiment by RCNP. Compared to other astrophysical constraints on the NS mass and radius, the allowed region that we have given in this study, based on nuclear experiments, still seems to be consistent, but the improvement in terrestrial experiments certainly helps us to understand the equation of state for NS matter. A number of future experiments are planned, which are expected to provide a further constraint on the NS mass and radius relation. For example, a CREX measurement with ^{48}Ca has already been done, which may tell us the additional constraint. In addition, the constraint on the higher-order saturation parameters, such as $K_{\rm sym}$ and Q_0, is also important for constraining the NS EOS; see, e.g., Ref. [63].

Acknowledgements

The authors are grateful to X. Roca-Maza and X. Viñas for giving us some data on L constraints in Fig. 1 and to A. Dohi for providing the data for the NICER constraint in Fig. 2. They also acknowledge R. Hirai, T. Isobe, K. Grande-Otsuki, D. Suzuki, and T. Takiwaki for fruitful discussions. This work is supported in part by JSPS KAKENHI (Grant Numbers: JP19J20543, JP19KK0354, JP19H00693, JP20H04753, JP20H05648, JP21H01087, JP21H01088), the RIKEN Pioneering Program for "Evolution of Matter in the Universe (r-EMU)", and the RIKEN Incentive Research Project.

References

[1] P. Demorest, T. Pennucci, S. Ransom, M. Roberts, and J. Hessels, Nature **467**, 1081 (2010).
[2] J. Antoniadis et al., Science **340**, 6131 (2013).
[3] H. T. Cromartie et al., Nat. Astron. **4**, 72 (2019).
[4] E. Annala, T. Gorda, A. Kurkela, and A. Vuorinen, Phys. Rev. Lett. **120**, 172703 (2018).
[5] A. W. Steiner, J. M. Lattimer, and E. F. Brown, Astrophys. J. Lett. **765**, L5 (2013).
[6] M. C. Miller et al., Astrophys. J. Lett. **887**, L24 (2019).
[7] T. E. Riley et al., Astrophys. J. Lett. **887**, L21 (2019).
[8] J. Estee et al., Phys. Rev. Lett. **126**, 162701 (2021).
[9] D. Adhikari et al., Phys. Rev. Lett. **126**, 172502 (2021).
[10] B. T. Reed, F. J. Fattoyev, C. J. Horowitz, and J. Piekarewicz, Phys. Rev. Lett. **126**, 172503 (2021).
[11] J. Zenihiro et al., Phys. Rev. C **82**, 044611 (2010).
[12] S. Shlomo, V. M. Kolomietz, and G. Colò, Eur. Phys. J. A **30**, 23 (2006).
[13] U. Garg and G. Colò, Prog. Part. Nucl. Phys. **101**, 55 (2018).
[14] X. Viñas, M. Centelles, X. Roca-Maza, and M. Warda, Eur. Phys. J. A **50**, 27 (2014).
[15] B.-A. Li, P. G. Krastev, D.-H. Wen, and N.-B. Zhang, Eur. Phys. J. A **55**, 117 (2019).
[16] S. Abrahamyan et al., Phys. Rev. Lett. **108**, 112502 (2012).
[17] P.-G. Reinhard, X. Roca-Maza, and W. Nazarewicz, Phys. Rev. Lett. **127**, 232501 (2021).
[18] X. Roca-Maza, M. Centelles, X. Vinas, and M. Warda, Phys. Rev. Lett. **106**, 252501 (2011).
[19] K. Hebeler, J. M. Lattimer, C. J. Pethick, and A. Schwenk, Phys. Rev. Lett. **105**, 161102 (2010).
[20] S. Gandolfi, J. Carlson, and S. Reddy, Phys. Rev. C **85**, 032801 (2012).
[21] M. Centelles, X. Roca-Maza, X. Viñas, and M. Warda, Phys. Rev. Lett. **102**, 122502 (2009).
[22] M. Warda, X. Viñas, X. Roca-Maza, and M. Centelles, Phys. Rev. C **80**, 024316 (2009).
[23] L.-W. Chen, C. M. Ko, B.-A. Li, and J. Xu, Phys. Rev. C **82**, 024321 (2010).
[24] S. Tagami, T. Wakasa, J. Matsui, M. Yahiro, and M. Takechi, Phys. Rev. C **104**, 024606 (2021).
[25] C. M. Tarbert et al., Phys. Rev. Lett. **112**, 242502 (2014).
[26] P. Möller, W. D. Myers, H. Sagawa, and S. Yoshida, Phys. Rev. Lett. **108**, 052501 (2012).
[27] P. Danielewicz, Nucl. Phys. A **727**, 233 (2003).
[28] B. K. Agrawal, J. N. De, and S. K. Samaddar, Phys. Rev. Lett. **109**, 262501 (2012).
[29] P. Danielewicz and J. Lee, Nucl. Phys. A **922**, 1 (2014).
[30] N. Paar, Ch. C. Moustakidis, T. Marketin, D. Vretenar, and G. A. Lalazissis, Phys. Rev. C **90**, 011304 (2014).
[31] X. Roca-Maza, L.-G. Cao, G. Colò, and H. Sagawa, Phys. Rev. C **94**, 044313 (2016).
[32] X. Roca-Maza and N. Paar, Prog. Part. Nucl. Phys. **101**, 96 (2018).
[33] M. A. Famiano et al., Phys. Rev. Lett. **97**, 052701 (2006).
[34] M. B. Tsang, Y. Zhang, P. Danielewicz, M. Famiano, Z. Li, W. G. Lynch, and A. W. Steiner, Phys. Rev. Lett. **102**, 122701 (2009).
[35] A. Klimkiewicz et al., Phys. Rev. C **76**, 051603 (2007).
[36] L. Trippa, G. Colò, and E. Vigezzi, Phys. Rev. C **77**, 061304 (2008).
[37] A. Carbone, G. Colò, A. Bracco, L.-G. Cao, P. F. Bortignon, F. Camera, and O. Wieland, Phys. Rev. C **81**, 041301 (2010).
[38] X. Roca-Maza, M. Brenna, B. K. Agrawal, P. F. Bortignon, G. Colò, L.-G. Cao, N. Paar, and D. Vretenar, Phys. Rev. C **87**, 034301 (2013).
[39] X. Roca-Maza, M. Centelles, X. Viñas, M. Brenna, G. Colò, B. K. Agrawal, N. Paar, J. Piekarewicz, and D. Vretenar, Phys. Rev. C **88**, 024316 (2013).
[40] X. Roca-Maza, X. Viñas, M. Centelles, B. K. Agrawal, G. Colò, N. Paar, J. Piekarewicz, and D. Vretenar, Phys. Rev. C **92**, 064304 (2015).
[41] C. Xu, B.-A. Li, and L.-W. Chen, Phys. Rev. C **82**, 054607 (2010).
[42] J. M. Lattimer and Y. Lim, Astrophys. J. **771**, 51 (2013).
[43] B.-A. Li and X. Han, Phys. Lett. B **727**, 276 (2013).
[44] M. Oertel, M. Hempel, T. Klähn, and S. Typel, Rev. Mod. Phys. **89**, 015007 (2017).
[45] A. W. Steiner, J. M. Lattimer, and E. F. Brown, Astrophys. J. **722**, 33 (2010).
[46] H. Sotani, K. Iida, and K. Oyamatsu, Mon. Not. R. Astron. Soc. **479**, 4735 (2018).
[47] H. Sotani, K. Iida, and K. Oyamatsu, Mon. Not. R. Astron. Soc. **489**, 3022 (2019).
[48] K. Oyamatsu, H. Sotani, and K. Iida, PoS **INPC2016**, 136 (2017).

[49] H. Sotani, K. Iida, K. Oyamatsu, and A. Ohnishi, Prog. Theor. Exp. Phys. **2014**, 051E01 (2014).
[50] E. Fonseca et al., Astrophys. J. Lett. **915**, L12 (2021).
[51] D. Blaschke, A. Ayriyan, D. E. Alvarez-Castillo, and H. Grigorian, Universe **6**, 81 (2020).
[52] T. E. Riley et al., Astrophys. J. Lett. **918**, L27 (2021).
[53] M. C. Miller et al., Astrophys. J. Lett. **918**, L28 (2021).
[54] J. M. Lattimer, Ann. Rev. Nucl. Part. Sci. **62**, 485 (2012).
[55] E. Chabanat, P. Bonche, P. Haensel, J. Meyer, and R. Schaeffer, Nucl. Phys. A **635**, 231 (1998).
[56] F. Douchin and P. Haensel, Astron. Astrophys. **380**, 151 (2001).
[57] H. S. Köhler, Nucl. Phys. A **258**, 301 (1976).
[58] P.-G. Reinhard and H. Flocard, Nucl. Phys. A **584**, 467 (1995).
[59] L. Bennour, P.-H. Heenen, P. Bonche, J. Dobaczewski, and H. Flocard, Phys. Rev. C **40**, 2834 (1989).
[60] S. Typel, Phys. Rev. C **89**, 064321 (2014).
[61] H. Shen, H. Toki, K. Oyamatsu, and K. Sumiyoshi, Nucl. Phys. A **637**, 435 (1998).
[62] H. Togashi, K. Nakazato, Y. Takehara, S. Yamamuro, H. Suzuki, and M. Takano, Nucl. Phys. A **961**, 78 (2017).
[63] H. Sotani and H. Togashi, Phys. Rev. D **105**, 063010 (2022).